AIAA 2001-1221

Modified Mode-I Cracked Sandwich Beam (CSB) Fracture Test

S.A. Smith
NASA Langley Research Center
Hampton, VA 23681

and

K.N. Shivakumar
Center for Composite Materials Research
North Carolina A&T State University
Greensboro, NC 24711

42nd AIAA/ASME/ASCE/AHS/ASC
Structures, Structural Dynamics, and Materials Conference
April 16-19, 2001/Seattle, WA

Modified Mode-I Cracked Sandwich Beam (CSB) Fracture Test

S.A. Smith*
NASA Langley Research Center
Hampton, Virginia
and
K.N. Shivakumar†
North Carolina A&T State University
Greensboro, North Carolina

Abstract

Five composite sandwich panels were fabricated using vacuum assisted resin transfer molding (VARTM). Four of these panels had E-glass/vinyl-ester facesheets and one had carbon/epoxy facesheets. The sandwich panels had different density PVC foam cores. The four E-glass panels had core densities of 80, 100, 130, 200 kg/m^3. The sandwich with carbon/epoxy facesheets had a core with density of 100 kg/m^3. Fracture tests were conducted using a modified Cracked Sandwich Beam (CSB) test configuration. Load-displacement curves were obtained for loading and unloading of the specimens during crack growth. Various increments of crack growth were monitored. Critical Strain Energy Release Rates (SERR) were determined from the tests using the area method. The critical values of SERR can be considered the fracture toughness of the sandwich material. The fracture toughness ranged 367 J/m^2 to 1350 J/m^2 over the range of core densities. These results are compared to the Mode-I fracture toughness of the PVC foam core materials and values obtained for foam-cored sandwiches using the TSD specimen. Finite-element analyses (FEA) were performed for the test configuration and Strain Energy Release Rates were calculated using the Virtual Crack Closure Technique (VCCT). The SERR values determined from the FEA were scaled to the fracture loads, or critical loads, obtained from the modified CSB tests. These critical loads were in close agreement with the test values.

Introduction

The interfacial fracture toughness of sandwich beams has received a great deal of attention in literature. Carlsson, et al [1] and Prasad and Carlsson [2-4] proposed several tests to investigate the Mode-I and Mode-II interfacial fracture toughness of sandwich materials. These tests include the Mode-I and Mode-II Cracked Sandwich Beam (CSB). Cantwell and Davies introduced the Single Cantilever Beam (SCB), a modified version of the Mode-I CSB where the specimen was placed on a rolling carriage [4,5]. Echtmeyer and McGeorge used the Mode-I CSB configuration but termed it the Non-symmetric Sandwich Split Beam (NSSB) [6]. Recently, several more specimens, including the Tilted Sandwich Debond (TSD), have been proposed to study mixed-mode fracture in sandwich beams [7-11]. In the current study a modified CSB test configuration is used. The CSB specimen is shown in figure 1. The mode-I CSB and the modified Mode-I CSB configurations are shown in figure 2. The proposed modification involves adding a roller support at the free end of the specimen to prevent large rotations.

The goal of the current study is to investigate the fracture toughness of sandwich materials fabricated using Vacuum Assisted Resin Transfer Molding (VARTM). The fabrication of the sandwich materials is presented first. This is followed by a description of the fracture testing and the presentation of the test results. The finite-element modeling of the modified

---

* Aerospace Engineer, Army Research Laboratory-Vehicle Technology Directorate, Member AIAA
† Director, Center for Composite Materials Research, Department of Mechanical Engineering, Associtae Fellow AIAA

Mode-I CSB configuration is described and the FEA results are compared to the test results.

Material Processing

Two different fiber reinforcements were selected for the sandwich panels. Four panels were processed with BGF 2532, a 1K plain-weave E-glass fabric with an areal weight of 237 g/m^2. One panel was processed with Cytec-Fiberite W-5-322, a 3K plain-weave T-300 carbon fabric that has an areal weight of 195 g/m^2. The matrix systems used were Dow Derakane 411-350 vinylester and SC-15 toughened epoxy by Applied Poleramic, Inc. The material properties of these constituent materials are listed in Table 1. The four E-glass sandwich panels were processed with the vinylester resin, while the carbon sandwich panel was processed with the toughened epoxy resin. The core materials used for the sandwich panels were Diab Divinycell H grade PVC foams. The core densities of the E-glass panels were 80, 100, 130, and 200 kg/m^3, respectively (H80/G, H100/G, H130/G and H200/G). The carbon/epoxy panel had a 100 kg/m^3 core (H100/C). All of the core materials were 25.4-mm thick.

Vacuum Assisted Resin Transfer Molding

A flat 13-mm thick aluminum plate measuring 762-mm wide by 1219-mm long was used as a mold surface for lay-up of the sandwich panels. The mold was treated with a release agent and the sandwich preform was placed onto the surface. The sandwich preform consisted of 12 layers reinforcement fabric stacked on top and bottom of the rigid, closed cell, PVC foam core. The preform measured 305-mm wide by 610-mm long. Peel plies were used on top and bottom of the preform. A greenhouse 50% shade cloth was stretched over the top and bottom peel plies to act as a distribution media. Vacuum sealant tape was placed around the perimeter of the mold surface and nylon film was used to cover the stacked material creating a sealed vacuum bag. A vacuum pump was used to evacuate the sealed bag. After evacuation, resin was allowed to flow into the preform at one end of the panel and across the distribution media to the vacuum port. Flow control was maintained through the use of a ball valve. The flow was cycled in one-minute increments to prevent the resin from entering the mold too quickly. The resin supply tubing was sealed after the preform was thoroughly wetted. The vacuum pump was then shut down and the vacuum port sealed. The consolidated preform was allowed to cure overnight at lab temperature (20 °C). The panels with vinyl-ester resin were post-cured for 2 hours at 100 °C. The panel infused with SC-15 resin was post cured for 4 hours at 60 °C followed by 4 hours at 100 °C.

Material Characterization

The fiber volume fractions of the facesheet materials were determined using the areal weight of the reinforcement fabric and the thickness of each panel. The average thickness, h, of each panel was determined from measurements at multiple locations. The sandwich thickness $h = 2t_s+t_c$, where t_s is the facesheet thickness and t_c is the core thickness. Hence, $t_s = (h-t_c)/2$. The volume, V, of a 1-mm unit cell of facesheet materials is t_s-mm^3. The fiber volume, V_f, of the unit cell of facesheet material is the areal weight of the reinforcing fabric times the number of layers of reinforcement divided by the fiber density. Thus, the fiber volume fraction v_f of a 1-mm unit cell of facesheet material is

$$v_f = \frac{V_f}{V} = \frac{n \times AW}{t_s \rho_f}. \qquad (1)$$

In the preceding expression, n is the number of layers of reinforcement fabric in the face sheet, AW is the areal weight of the reinforcement fabric in kg/mm^2, and ρ_f is the density of the fiber in the reinforcement fabric in kg/mm^3. The average thickness of the panels and the calculated fiber volume fractions are shown in Table 2. The fiber volume fractions, the mechanical properties of the neat resin and fiber reinforcement, and the textile configuration were used as input to a laminated textile composite analysis code, mmTexlam [12]. The properties of the neat resin and fiber reinforcement are shown in Table 1. The material properties calculated for the facesheets are presented in Table 2. The properties of the different density PVC foam core materials are shown in Table 3.

Fracture Testing

Figure 1 shows the configuration of a CSB specimen. Five CSB specimens, similar to the specimen shown in figure 3, were machined from the each of the sandwich panels. The specimens were cut from the panels using a water-cooled tile saw with a diamond-coated blade. The nominal length and width of the specimens were 38.1-mm and 254-mm, respectively.

Specimen Preparation

After machining the CSB specimens to their final dimensions aluminum piano hinges were adhesively bonded to the facesheets. These hinges facilitate loading of the CSB specimen and are shown as tabs in figures 1 and 3. The hinges are mounted 25.4-mm from the end of the specimen. The mounting procedure involved abrading surfaces of both the facesheet and the hinge. The abraded areas are rinsed with acetone and allowed to air dry. The hinges were bonded to the facesheets using 3M DP-460 two-part epoxy adhesive. To maintain bond-line thickness 1 μ glass beads were added to the adhesive in proportions of 5% by weight. The glass beads were mixed into epoxy at the same time part A (base resin) and part B (hardener) were combined. After mixing, the epoxy was spread onto the aluminum tabs (piano-hinges), which were aligned on the specimens and clamped in place. The adhesive was then cured at 60 °C for 2 hours. A delamination was cut into the interface region using a thin coping saw to approach initial crack length. A surgical knife was used to reach the desired initial crack length (25.4-mm). White paint was applied along the interface ahead of the crack front to facilitate the tracking of the crack-tip. Marked increments were place at 6.35-mm intervals along the interface region. The hinges (tabs), initial crack, paint, and crack growth increments are shown on a typical specimen in figure 3.

Test Procedure

The fracture tests were carried out on a 50-kip MTS test machine using a 1-kip load cell. The piano hinge tabs of the CSB specimen were mounted in the hydraulic grips of the load frame. A roller support was mounted on the load frame to prevent the specimen from rotating. This support is shown schematically in figure 2 and on the actual load frame in figure 4. An optical tracking microscope was used to locate and track the crack tip. The crack tip location was recorded at the start of each test. A picture of the test configuration is shown in figure 4.

The tests were conducted in displacement control with a crosshead displacement rate of 1.3-mm/min. Load and crosshead displacement were recorded throughout the test. Once the test had been started, the crack tip was monitored for growth. The crack was allowed to grow steadily until it extended 25.4-mm or unsteady growth occurred. If the crack grew in a steady manner, the crack progression was monitored and flag was placed in the data file each time the crack-tip passed through the 6.35-mm intervals marked on the specimen. The crack was allowed to grow approximately 25.4-mm and then the crosshead displacement was reversed. Unloading data was recorded. If the crack grew in an unstable fashion, the crosshead displacement was stopped, the new crack tip location was found and recorded, and then the crosshead displacement was reversed. Again, unloading data was recorded. This procedure was repeated over approximately 102-mm of crack growth.

Computation of Fracture Toughness

The Strain Energy Release Rate (SERR) can be calculated from the load and displacement values obtained during a fracture test using the area method [13]. The area under a single load/unload cycle was calculated using the trapezoid rule. The area, ΔE, corresponds to the energy-released as the crack grows. The critical SERR, or fracture toughness (G_c), can be obtained using

$$G_c = \frac{\Delta E}{b\,\Delta a}. \qquad (2)$$

In the preceding expression ΔE is the area under the load-displacement curve, Δa is the crack extension noted during the test, and b is the width of the specimen. This value was taken as the average energy released for a crack extension Δa. The procedure is repeated for each loading/unloading cycle or between indicated critical load values. Hence, several values can be obtained from a single test specimen.

Test Results

The load-displacement curves for typical specimens of H80/G, H100/G, H100/C, H130/G, and H200/G are shown in figures 5-9 respectively. In figures 5-7 (core densities of 80 and 100 kg/m^3), the load increases in gradual fashion until it reaches some critical value and sudden crack growth occurs. When the crack grows the load drops sharply. If the test were allowed to continue, the load would again rise gradually and then drop sharply with crack growth. This is referred to as stick-slip growth. The higher density cores (130-200 kg/m^3) did not exhibit this behavior. In the higher density cores the crack growth was steady and the load dropped gradually as the crack grew (Figs. 8 and 9). In figures 8 and 9 the data points represent the critical loads where the crack-tip traversed the 6.35-mm intervals marked on the specimens.

As noted previously, typical load-displacement values are shown in figures 5-9. The critical strain energy release rates were calculated from multiple tests

of the five specimens from each panel. Examples of the areas used in calculating G_c are shown in figures 10 and 11. Figure 10 is an example of the area used for stick-slip growth. Figure 11 is an example of an incremental area used for steady crack growth. The results from the area method calculations are plotted against crack length in figures 12-16 for panels H80/G, H100/G, H100/C, H130/G, and H200/G, respectively. Plotted with the test results are the mean value from the tests and upper and lower bounds located at plus or minus one standard deviation from the mean. Note that the values are nearly constant over the range of crack lengths. Also note that the values from the H100/G panel (E-glass/vinylester facesheets) and the H100/C panel (carbon/epoxy facesheets) are nearly identical. These two panels have identical core materials but different facesheet materials. This suggests that the fracture toughness is independent of the facesheet material, or resin used in fabrication. The data-scatter appears larger for the higher density cores. However, the coefficient of variation is around 0.20 for all the tests. The mean critical energy release rate was taken to be the fracture toughness for each sandwich panel. The mean values of fracture toughness and the coefficients of variation are presented in Table 4.

The fracture toughness values determined using the modified CSB fracture test configuration are plotted against core density in figure 17. Plotted with these values are the Mode-I fracture toughness values for the PVC foam cores and sandwich fracture toughness values determined by Carlsson from SENB and TSD tests [14]. Also plotted in figure 17 are trend lines for the modified CSB test values and upper and lower bounds located at one standard deviation form the trend line. Note that the CSB values and TSD values are in close agreement at densities of 80 kg/m^3 and 200 kg/m^3. The values determined in the current study and Carlsson's TSD values are significantly higher than the Mode-I fracture toughness of the core material, but follow the same increasing trend with core density. This suggests that conservative damage-tolerant design of foam core sandwich materials could be based on the Mode-I fracture toughness of the core material.

Finite Element Analysis

Finite-element models were created for the modified CSB test configuration with crack lengths of 25.4, 50.8, 76.2 and 101.6-mm. An example of a coarse finite-element mesh is shown in figure 18. A similar but refined version was used to evaluate the modified CSB configurations. The refined model consisted of 31681 nodes and 31200 elements. Four-node quadrilateral elements with bilinear shape functions were used. The element size at the crack tip was 1% of the crack length modeled. The boundary conditions for the modified CSB test configuration are

$$u(0,0)=0,\ v(0,0)=0,$$

$$u(0,2t_s+t_c)=0,$$

and

$$v(\ell,2t_s+t_c)=0.$$

A unit load, P=1 N, was applied the positive y-direction at the node $(0,2t_s+t_c)$. The boundary conditions and applied load are shown in figure 2. The material properties used in the model are given in Tables 2 and 3. The facesheets were modeled as orthotropic while the core was modeled as isotropic.

A plain-strain finite-element analysis was conducted for each crack length model. The SERR was calculated for each model using the Virtual Crack Closure Technique [15]. A critical load was determined for the model by scaling the SERR obtained numerically to the critical value obtained from the tests. The critical load P_{cr} is calculated using

$$P_{cr}=\sqrt{\frac{G_c}{G_{FEA}}}. \qquad (3)$$

Where G_c is the fracture toughness obtained from fracture testing and G_{FEA} is the value of SERR obtained from the finite-element analysis.

The values of P_{cr} obtained from the scaling the finite-element results are plotted against crack length in figures 19-23. Plotted with the scaled values from the FEA are the critical load values from the fracture tests and the trend line. The finite-element scaled values are in close agreement with all of the tests. The largest difference is noted for the H100/G panel (E-glass/vinylester facesheet with 100 kg/m^3 core). It is not clear why the values differed more significantly from the tests for this panel. However, if the lower bound on the fracture toughness were used in the scaling of the SERR it is clear FEA could conservatively predict the critical load for a given flaw size.

Concluding Remarks

Fracture toughness of VARTM PVC foam core sandwich structures was investigated using a modified Mode-I Cracked Sandwich Beam fracture test configuration. The sandwich structures had foam core

densities of 80, 100, 130, 200 kg/m^3, respectively. The fracture toughness values obtained for the sandwich panels were in close agreement with values in literature for panels with the same core materials. The test results indicate the fracture toughness is independent of crack length and constant over nearly 102-mm crack growth. Also the fracture toughness was not dependant on the facesheet material. Sandwich panels with identical cores but different face sheets had nearly identical values of fracture toughness. It was also noted that the sandwich fracture toughness values were significantly higher than the Mode-I toughness of the core materials. This suggests that Mode-I fracture toughness of the core could be used for conservative damage-tolerant design of foam core sandwich structures. Two-dimensional finite-element models of the modified Mode-I CSB test were able to reproduce the critical load values obtained from the fracture tests.

Acknowledgments

This research was supported by NASA Langley Research Center and the Office of Naval Research under grant No.(s) NAG1-1956 and N00014-99-0445.

References

1. L.A. Carlsson, L.S. Sendlein, and S.L. Merry, "Characterization of Facesheet/Core Shear Fracture of Composite Sandwich Beams," *Journal of Composite Materials*, Vol. 25, 1991, pp. 101-116
2. Leif A. Carlsson and Srinivas Prasad, "Interfacial Fracture of Sandwich Beams," *Engineering Fracture Mechanics*, Vol. 44, No. 4, 1993, pp. 581-590
3. Srinivas Prasad and Leif A. Carlson, "Debonding and Crack Kinking in Foam Core Sandwich Beams-I. Analysis of Fracture Specimens," *Engineering Fracture Mechanics*, Vol. 47, Nov. 6, 1994, pp 813-824
4. Srinivas Prasad and Leif A. Carlsson, "Debonding and Crack Kinking in Foam Core Sandwich Beams-II. Experimental Investigation," *Engineering Fracture Mechanics*, Vol. 47, No. 6, 1994, pp. 825-841
5. W.J. Cantwell and P. Davies, "A Test Technique for Assessing Core-Skin Adhesion in Composite Sandwich Structures," *Journal of Material Science Letters*, Vol. 13, 1994, pp. 203-205
6. W.J. Cantwell and P. Davies, "A Study of Skin Core Adhesion in Glass Fibre Reinforced Sandwich Materials," *Applied Composite Materilas*, No. 3, 1996, pp. 407-420
7. A.T. Echtermeyer and D. McGeorge, "Fracture Toughness of Core Skin Interfaces of Sandwich Materials," *Proceedings of the Fourth International Conference on Sandwich Construction*, Vol. 2, 1998, pp. 635-646
8. Xiaming Li, and Leif A. Carlsson, "A Test Specimen for Determining The Fracture Resistance of a Facing Core Interface," *Proceedings of the Fourth International Conference on Sandwich Construction*, Vol. 2, 1998, pp. 646-658
9. Xiaming Li, and Leif A. Carlsson, "The Tilted Sandwich Debond (TSD) Specimen for Face/Core Interface Fracture Characterization," *Journal of Sandwich Structures and Materials*, Vo. 1, 1999, pp. 60-75
10. L.D. McGarva and B.T. Aström, "Experimental Investigation of Compression Moulding of Glass/PA12-PMI Foam Core Sandwich Components," *Composites: Part A*, Vol. 30, 1999, pp 1171-1185
11. W.J. Cantwell, et al., "Interfacial Fracture in Sandwich Laminates," *Composites Science and Techology*, Vol. 59, 1999, pp. 2079-2085
12. K. N. Shivakumar, P. Challa, and D. R. Reddy, "mmTexlam – A Graphical User Interfaced Code for Laminated Textile Composites," *42nd AIAA/ASME/ASCE/AHS/ASC Structures, Structural Dynamics, and Materials Conference*, AIAA Paper No. 2001-1571, 2001
13. T.L. Anderson, "Fracture Mechanics: Fundamentals and Applications," Second Edition, CRC press, NewYork, 1995, p. 450
14. Leif Carlsson, Facsimile communication, March 2001
15. Rybicki and Kanninen, "A Finite-Element Calculation of Stress-Intensity factors by a Modified Crack Closure Integral," *Engineering Fracture Mechanics*, Vo. 9, pp. 931-938

Table 1. Mechanical properties of facesheet constituent materials

	E-glass	T-300	411-350	SC-15
Density, g/cm^3	2.57	1.76	1.12	1.10
E_{xx}, GPa	72.50	231.7	3.38	2.82
E_{yy}, GPa	-	13.79	-	-
ν_{xy}	0.20	0.20	0.35	0.40
G_{xy}, GPa	30.21	8.96	1.41	2.70

Table 2. Mechanical properties calculated for the facesheet materials

	H80/G	H100/G	H100/C	H130/G	H200/G
Sandwich thickness, mm	30.89	32.04	30.85	31.97	29.32
Fiber volume fraction	0.40	0.33	0.49	0.34	0.56
E_{xx}, GPa	20.60	17.02	58.12	17.53	27.59
E_{yy}, GPa	10.70	8.52	8.45	8.82	13.95
ν_{xy}	0.33	0.36	0.44	0.36	0.31
G_{xy}, GPa	3.69	2.91	2.70	2.78	4.91

Table 3. Mechanical properties of core materials

	H80	H100	H130	H200
Density, kg/m^3	80	100	130	200
E_{xx}, MPa	80	105	140	230
ν_{xy}	0.29	0.31	0.35	0.35
G_{xy}, MPa	31	40	52	85

Table 4. Fracture toughness of foam core sandwich panels

Core Density kg/m^3	G_c J/m^2	Coefficient of Variation
80	367	0.16
100	558	0.19
130	878	0.24
200	1350	0.20

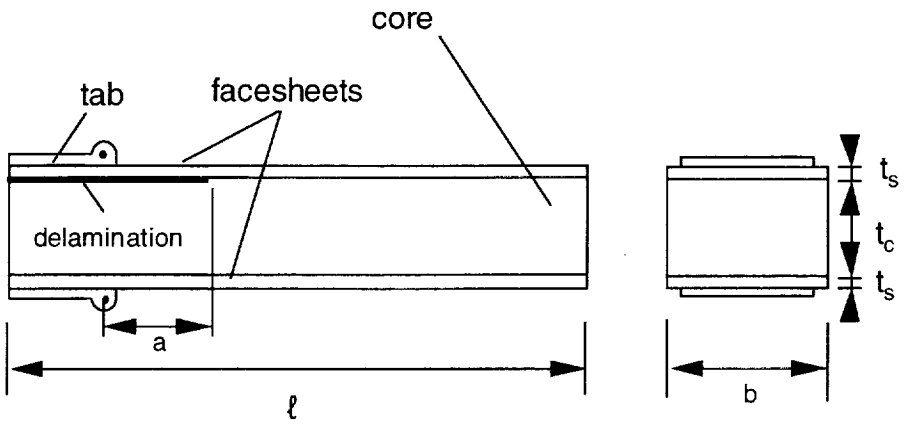

Figure 1. Mode-I Cracked Sandwich Beam (CSB) specimen configuration

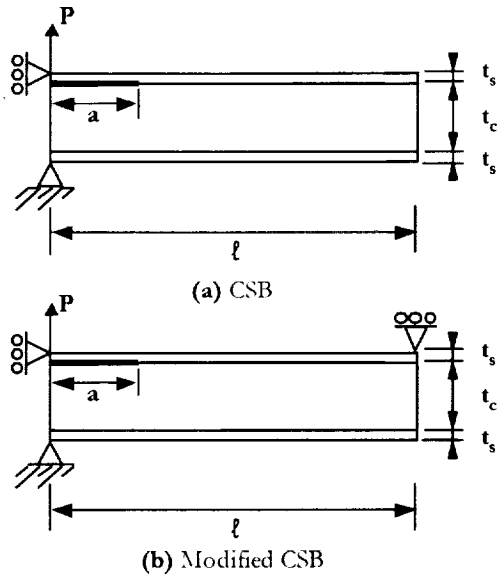

Figure 2. Mode-I CSB and modified Mode-I CSB fracture test configurations

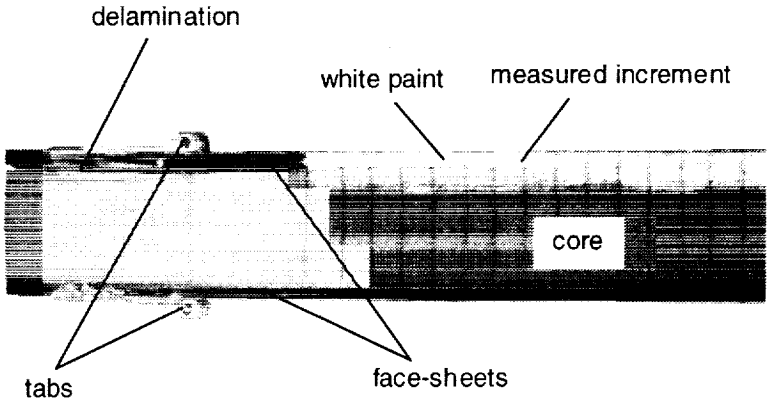

Figure 3. Typical Mode-I Cracked Sandwich Beam (CSB) fracture test specimen

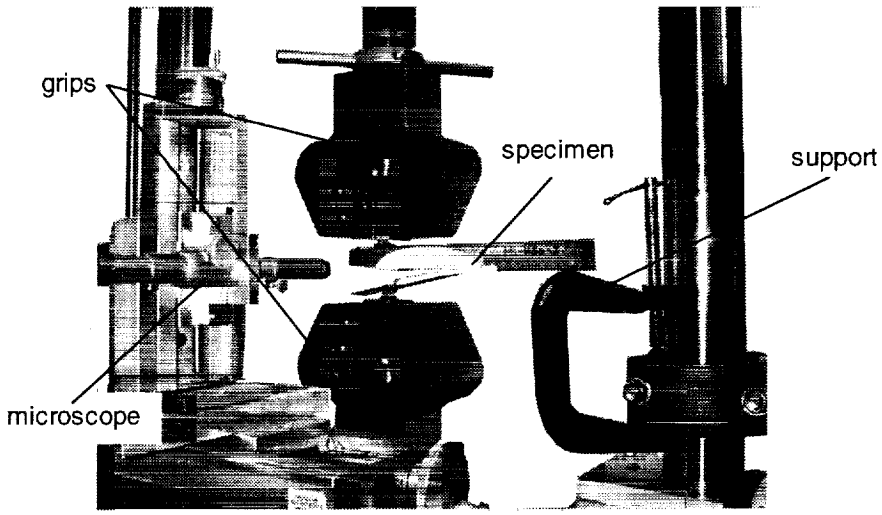

Figure 4. The modified Mode-I Cracked Sandwich Beam (CSB) fracture test

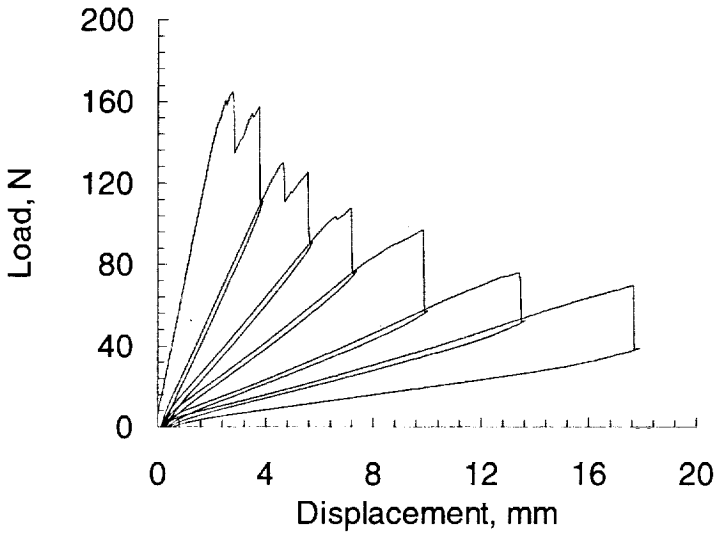

Figure 5. Load-displacement response of modified CSB test specimen (H80/G)

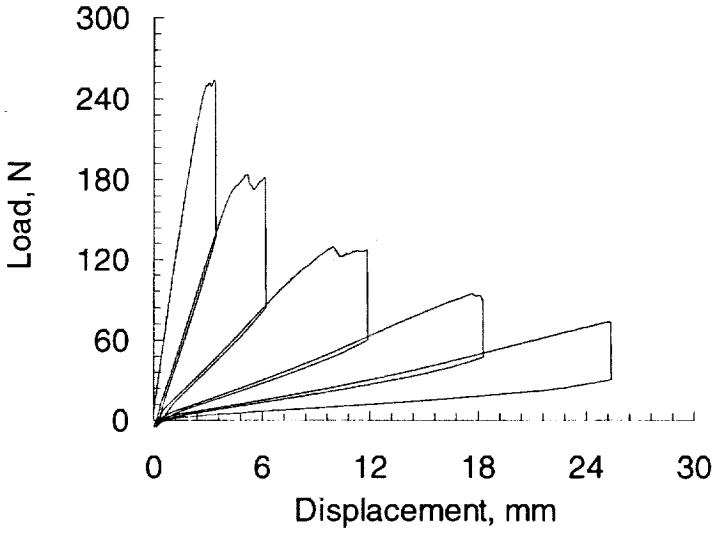

Figure 6. Load-displacement response of a modified CSB test specimen (H100/G)

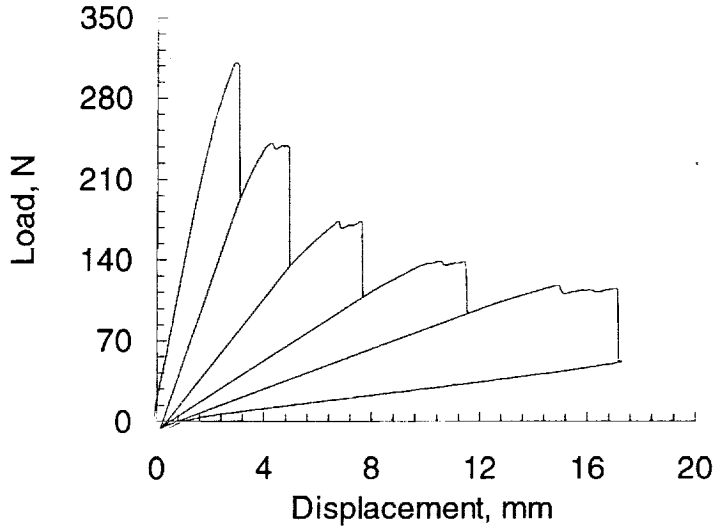

Figure 7. Typical load-displacement response of a modified CSB test specimen (H100/C)

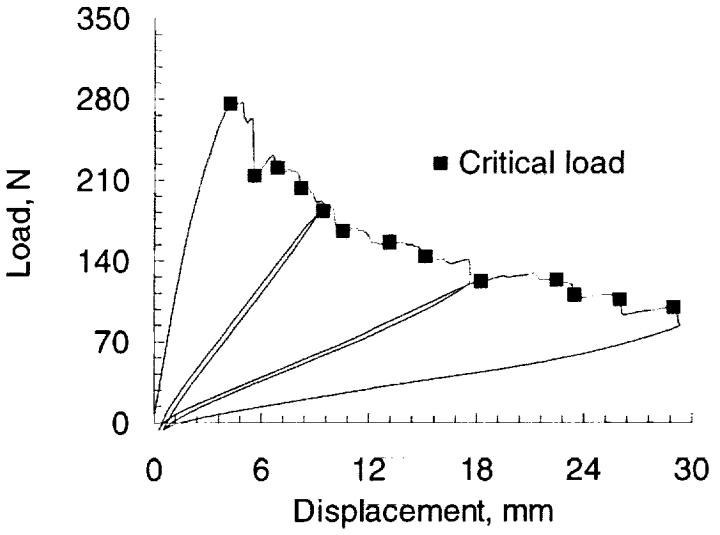

Figure 8. Load-displacement response of a modified CSB test specimen (H130/G)

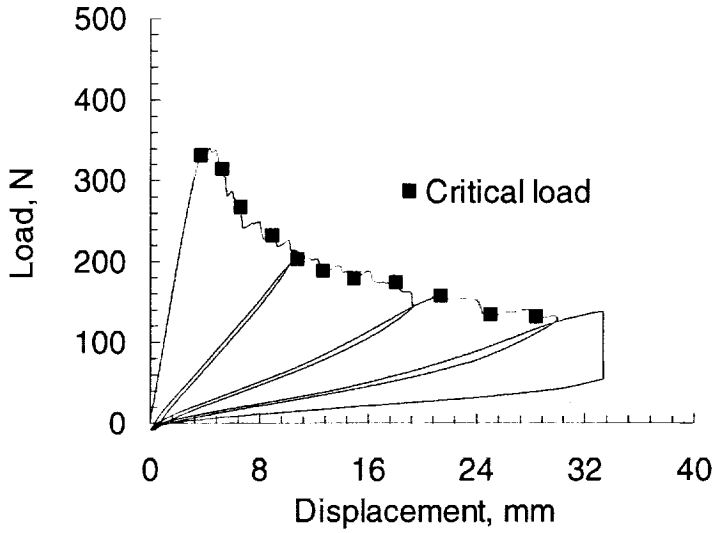

Figure 9. Load-displacement response of modified CSB test specimen H200/G-5

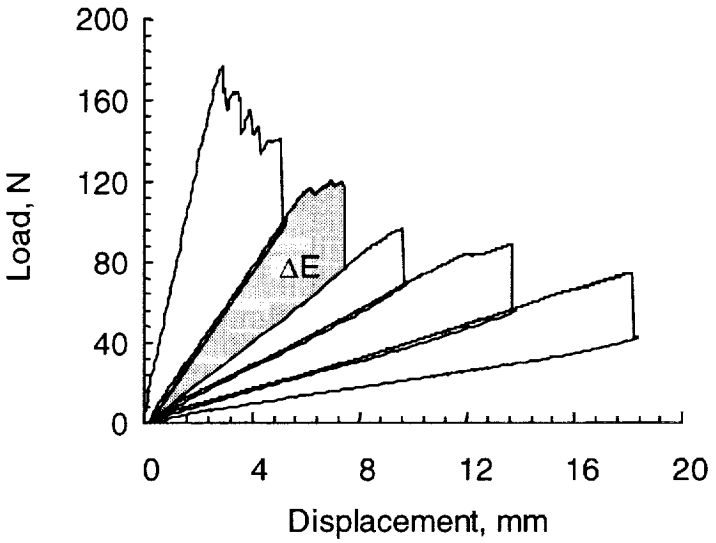

Figure 10. Determination of area used in calculating strain energy release rate for stick-slip crack growth

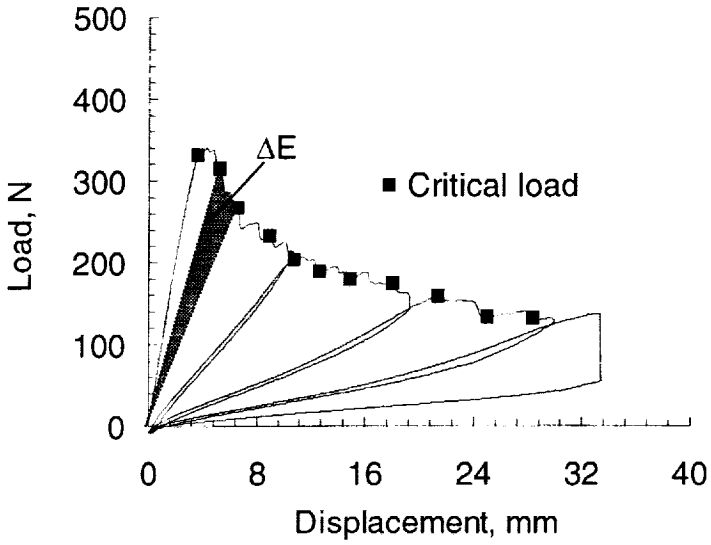

Figure 11. Determination of area used in calculating strain energy release rate for steady crack growth

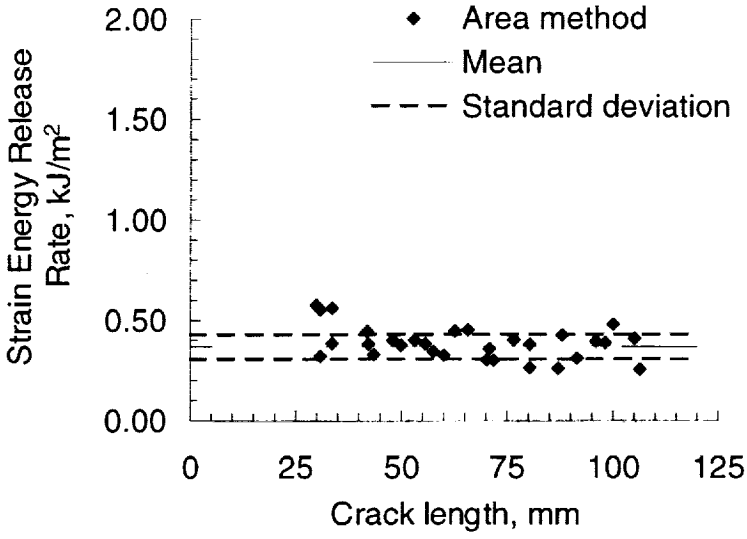

Figure 12. Critical Strain Energy Release Rate for various crack lengths (H80/G)

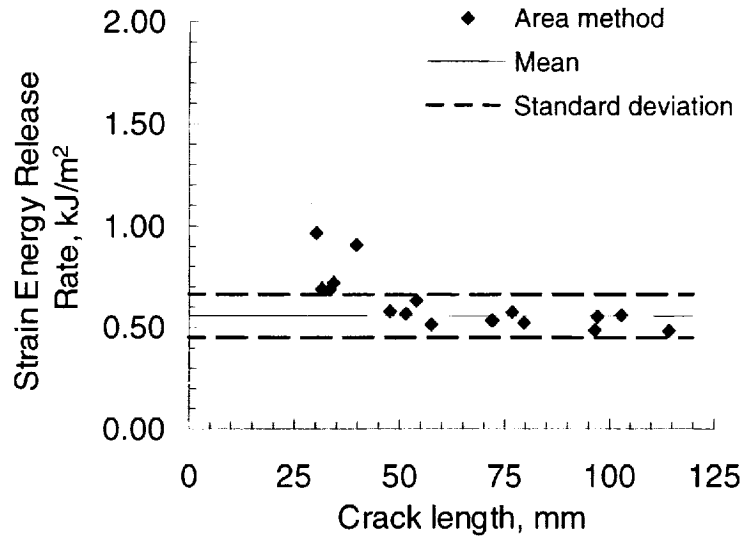

Figure 13. Critical Strain Energy Release Rate for various crack lengths (H100/G)

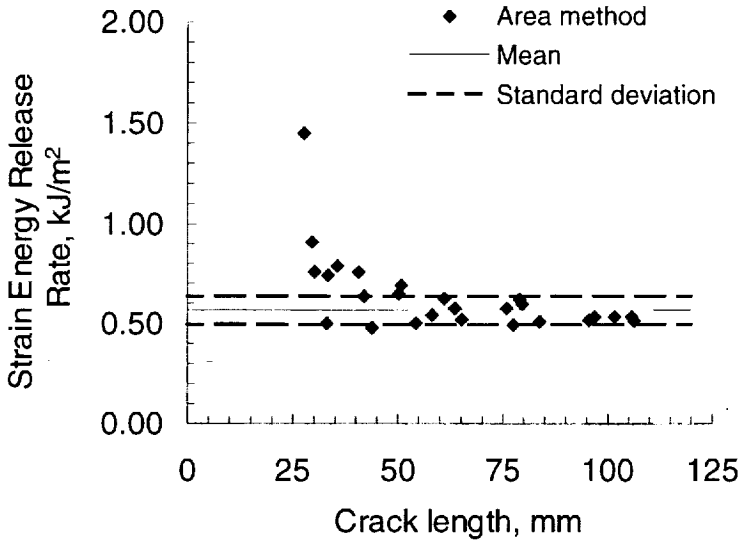

Figure 14. Critical Strain Energy Release Rate for various crack lengths (H100/C)

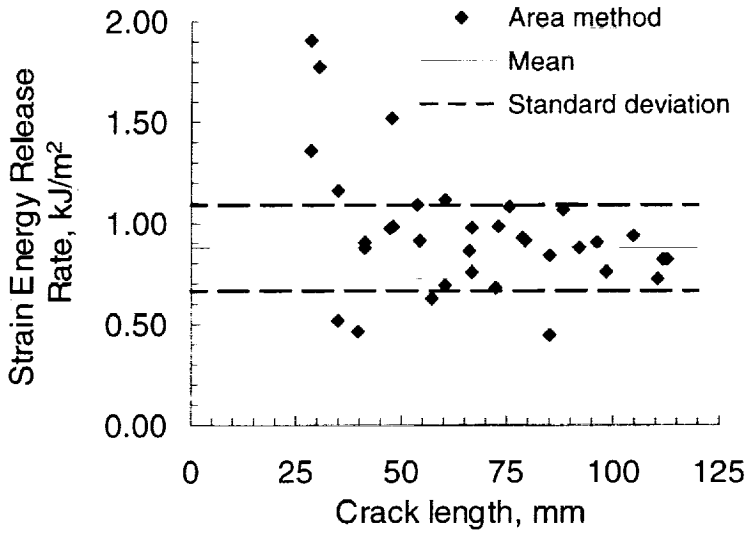

Figure 15. Critical Strain Energy Release Rate for various crack lengths (H130/G)

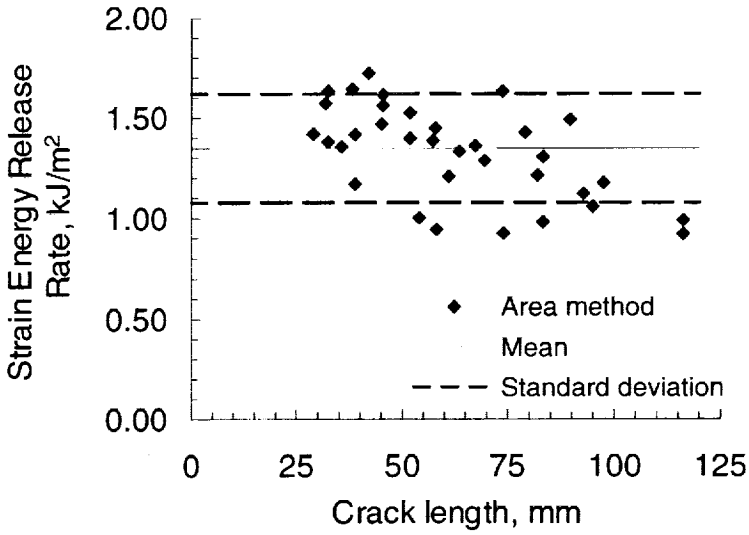

Figure 16. Critical Strain Energy Release Rate for various crack lengths (H200/G)

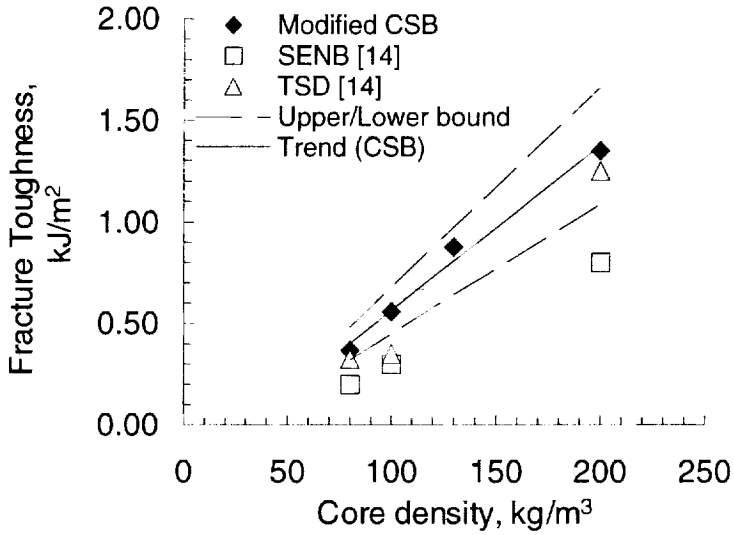

Figure 17. Variation of fracture toughness with core density

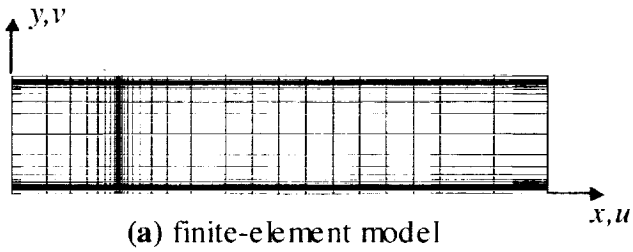

(a) finite-element model

(b) deformed shape

Figure 18. Finite-element modeling of modified CSB test

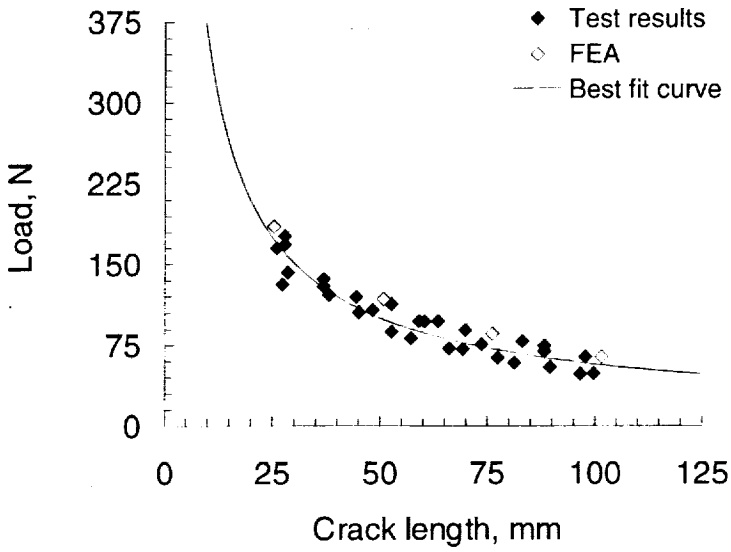

Figure 19. Critical load for modified CSB test specimens (H80/G)

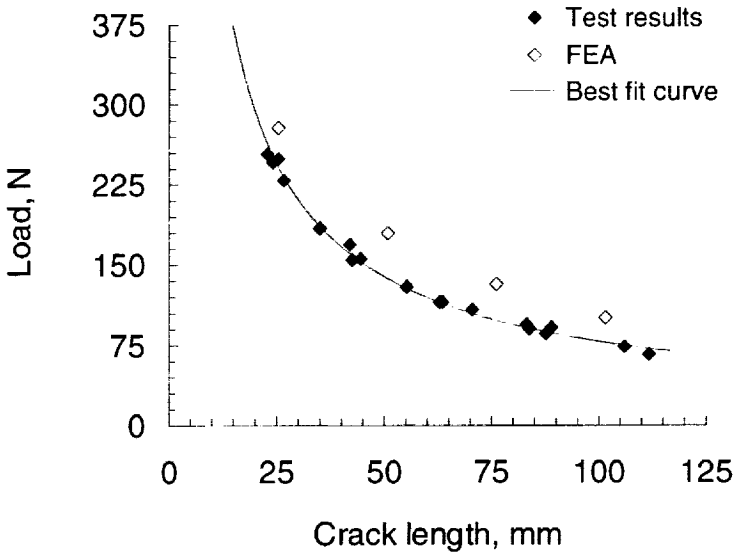

Figure 20. Critical load for modified CSB test specimens (H100/G)

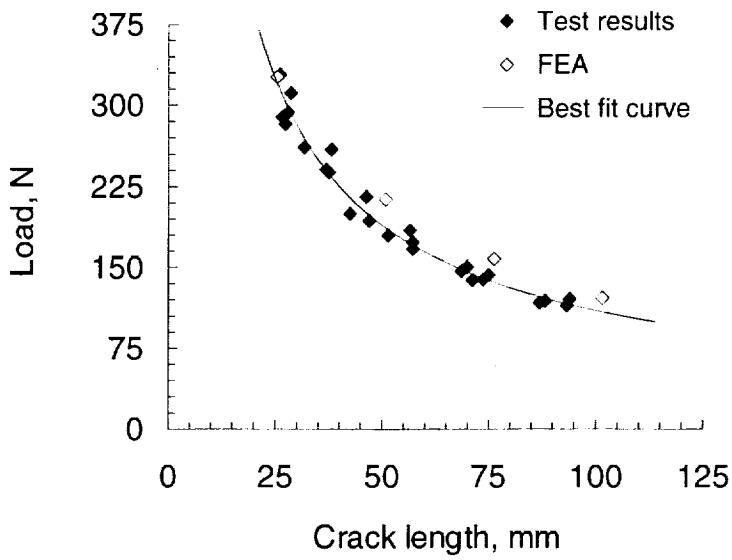

Figure 21. Critical load for modified CSB test specimens (H100/C)

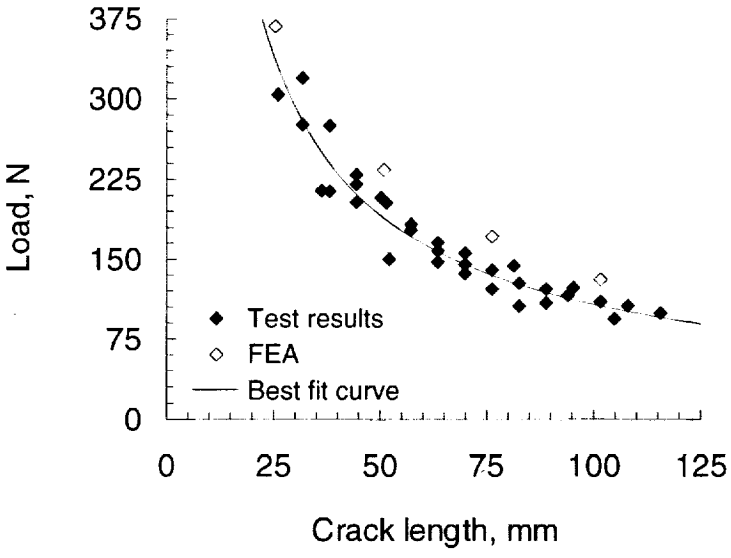

Figure 22. Critical load for modified CSB test specimens (H130/G)

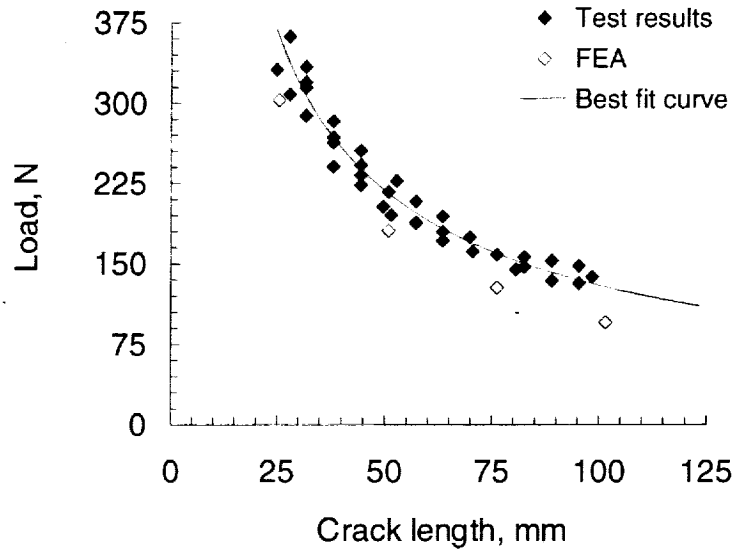

Figure 23. Critical load for modified CSB test specimens (H200/G)